ASPS Conference Proceedings 1: 1293-1297 (2022)

Proceedings of

12th Structural Engineering Convention-An International Event (SEC 2022)

Available at https://asps-journals.com/index.php/acp

# Effect of Horizontal Curve on the Response of Road Tunnels under Internal Explosion

Jagriti Mandal [1, *], Manmohan Dass Goel [2] and Ajay Kumar Agarwal [1]

[1] Department of Mining Engineering, Visvesvaraya National Institute of Technology, Nagpur – 440 010, India
[2] Department of Applied Mechanics, Visvesvaraya National Institute of Technology, Nagpur – 440 010, India

**Paper ID - 100188**

**Abstract**

Internal explosion in a tunnel is a complex loading phenomenon where the tunnel lining is subjected to not only direct impact of explosion but also loading due to multiple reflection of blast waves which could be of magnitude higher than that of incident blast wave. This kind of loading is complex in nature and difficult to predict using simple analysis tools. Further, it poses a serious threat to its structural integrity. Studies have been conducted in the past to understand the behaviour of tunnel under internal explosion. However, they have been focused on straight tunnels ignoring the convex and concave shapes introduced due to horizontal and vertical curves. Shape of the target surface has significant effect on the characteristics of blast wave. This study investigates the effect of horizontal curves on the damage behaviour of tunnel lining due to internal explosion. A series of numerical simulation are performed on box-shaped tunnel with varying curvature radius and the results are compared with that of straight tunnel adopting Multi-Material Arbitrary Lagrangian-Eulerian (MM-ALE) method using LS-DYNA®. Explosive and air are modeled using ALE formulation, whereas, tunnel and soil are modeled using Lagrangian formulation. Further, Jones-Wilkins-Lee equation of state is used to model the explosion. Damage to the tunnel lining is measured in terms of peak particle velocity (PPV) and von-Mises stress. It is observed that walls of curved tunnels undergo more PPV compared with straight tunnel wherein concave wall show the highest PPV. Propagation of blast wave along the tunnel length is significantly affected due to the introduction of curvature resulting in change in reflection patterns. This further leads to variation in stress contours on tunnel lining with higher concentration of stress in curved tunnels than in straight tunnel.

*Keywords*: Internal blast, tunnel, horizontal curve, blast response, FE, MM-ALE

## 1. Introduction

Underground facilities have become an integral part of our country's ever-growing infrastructure industry. Tunnels are among the most constructed underground structures since it has solved the problem of connectivity to remote regions with difficult terrains which were otherwise inaccessible. However, they have also been put under the potential threat of terrorist and accidental explosions. An explosion can release a blast wave that is capable of generating loading in the strain rate range of $10^4$-$10^6$ $s^{-1}$. Such a kind of loading which is transient, highly non-linear, and dynamic can cause severe damage to the structure. A blast wave is prone to amplification of its magnitude when it gets reflected by a surface. The amplification can reach a factor of 13 depending on the incident angle and characteristics of the target surface. An internal explosion in tunnel provides infinite possibilities of multiple reflections of blast wave which could lead to a drastic increase in load application on the tunnel lining. This necessitates a detailed analysis of blast phenomenon involved in the internal blast and its interaction with the tunnel and surrounding soil which could help in adopting effective mitigation measures.

Studies on understanding the effects of internal blast on tunnel have been carried out in the past which included detailed parametric studies [1-5]. However, most of the studies are focused on a straight segment of the tunnel neglecting the curvature aspect of the structure.

This study investigates the effect of horizontal curves on the damage behaviour of tunnel lining due to internal explosion. A series of numerical simulations are performed on box-shaped tunnel with varying curvature radius and the results are compared with that of straight tunnel adopting Multi-Material Arbitrary Lagrangian-Eulerian (MM-ALE) method using LS-DYNA® [6].

## 2. Geometrical Details

A box-shaped tunnel of cross-sectional dimensions of 5 m × 5 m, lining thickness of 300 mm, and length ($L$) of 20 m is considered for the study. One case of a straight tunnel and three cases of a curved tunnel with varying angle of curvature is taken. Three angles of curvature (θ) chosen for the investigation are 20°, 25°, and 30°. The radius of curvature ($R$) is calculated accordingly based on the chosen angle of curvature and maintaining a design speed of 50-60 km/hour and a safe sight distance of 35-50 m [7]. Explosion is located at the centre of the tunnel cross-section. Fig. 1 illustrates the schematic diagram of the tunnel.

*Corresponding author. Tel: +918551974970; E-mail address: jagritimandal@students.vnit.ac.in

Proceedings of the 12th Structural Engineering Convention (SEC 2022), NCDMM, MNIT Jaipur, India| 19-22 December, 2022



Published online: December 19, 2022
doi:10.38208/acp.v1.653

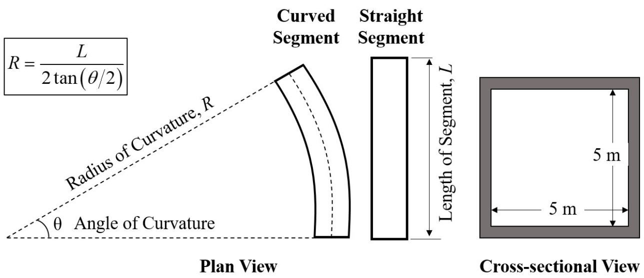


Fig. 1. Geometrical details of the tunnel

## 3. Finite Element Modelling

The finite element model of the defined problem is developed using LS-DYNA® [6]. Constant stress solid element of the global size of 150 mm with reduced integration is used with hourglass control based on Flanagan-Belytschko stiffness form. Tunnel and soil are modeled using Lagrangian element formulation. Whereas, the air and the explosive are modeled using arbitrary Eulerian-Lagrangian element formulation. A Mesh convergence study has been done to determine the mesh size appropriate for an accurate and time-efficient analysis. Symmetrical boundary conditions (SBC) are applied on two sides of the model and non-reflecting boundary conditions (NRBC) on the other outer sides of the model as shown in Fig. 2.

The lining of tunnels is often made of reinforced concrete. Under dynamic loading like a blast, they display non-linear behaviour as well as strain rate dependence. However, the study has ignored the strain rate-dependent behaviour of reinforced concrete in order to keep the numerical simulation simplistic and time-efficient. Using the principle of equivalent, concrete and reinforcement are assumed to be one single monolithic part. Plastic Kinematic material model is used to define the behaviour of reinforced concrete with parameters listed in Table 1.

This model is suitable for simulating soft soil under high strain rate loading. The compression of soil is predicted using a hydrostatic compression curve, the data of which along with other necessary material parameters are given in Fig. 3.

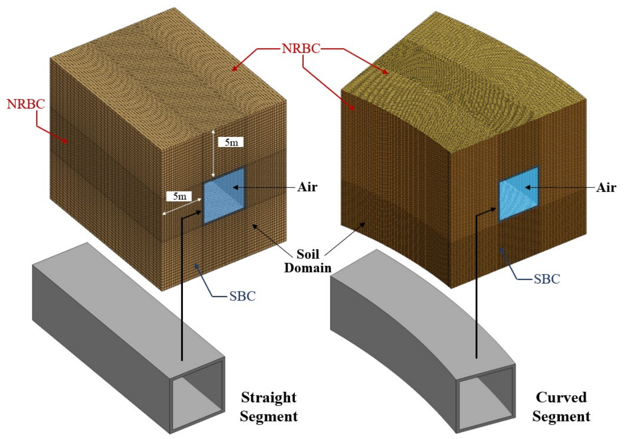


Fig. 2. Finite element model of the tunnel

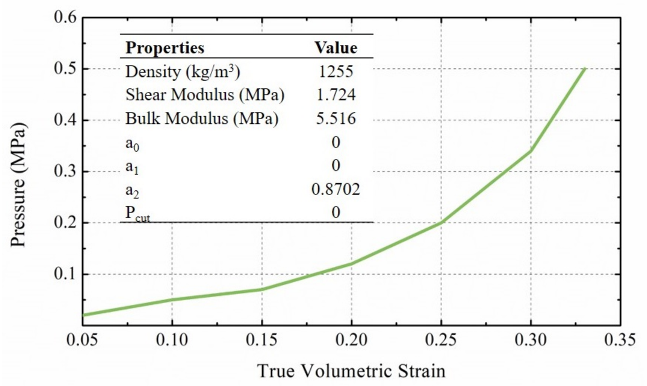


Fig. 3. Material parameters and hydrostatic compression curve of soil [9]

The air domain is modeled using the null material model, and the pressure is defined in terms of volume and internal energy using a linear polynomial equation of state. The pressure (P) is calculated using the expression,

$$P = C_0 + C_1\mu + C_2\mu^2 + C_3\mu^3 + \left(C_4 + C_5\mu + C_6\mu^2\right)E \quad (1)$$

This equation is modified by substituting the constants $C_0$, $C_1$, $C_2$, $C_3$, and $C_6$ with zero and $C_4$ and $C_5$ with $(\gamma - 1)$,

$$P = (\gamma - 1)\frac{\rho}{\rho_0}E \quad (2)$$

Where, $E$ = 0.25 MPa is the internal energy per initial volume, ρ is the relative density of air, $\rho_0$ =1 is the initial density of air, and γ = 1.4 is the ratio of specific heat. The density of air is taken as 1.29 kg/m$^3$ [9].

The explosive has been modeled using the high explosive burn material model, which makes use of variables including density (ρ = 1630 kg/m$^3$), detonation velocity ($v_D$ = 6930 m/s), and Chapman-Jouguet pressure ($P_{cut} = 2.1\times10^4$ MPa). The pressure is expressed in terms of relative density ($V$ = 1) and internal energy per starting volume ($E$ = 6000 MPa) using the Jones-Wilkins-Lee equation of state, and the expression is as follows:

$$p = A\left(1 - \frac{\omega}{R_1 V}\right)e^{-R_1 V} + B\left(1 - \frac{\omega}{R_2 V}\right)e^{-R_2 V} + \frac{\omega E}{V} \quad (3)$$

where ω = 0.35, $A = 3.738\times10^5$ MPa, $B = 3.747\times10^3$ MPa, $R_1$ = 4.15 and $R_2$ = 0.9 are JWL parameters and they depend of the type of explosive [9].

Table-1. Material properties for tunnel lining (Reinforced concrete) [8]

| Parameter | Value |
|---|---|
| Density (kg/m$^3$) | 2650 |
| Young's Modulus (GPa) | 39.1 |
| Poisson's Ratio | 0.25 |
| Yield Strength (MPa) | 100 |
| Tangent Modulus (MPa) | 4000 |
| Hardening Coefficient | 0.5 |
| Effective Plastic Strain | 0.8 |

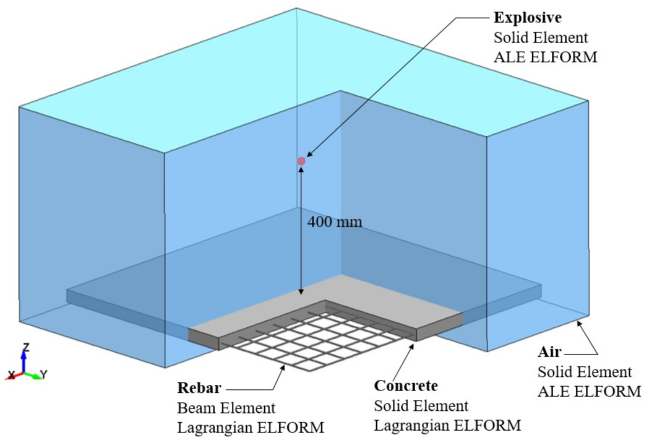


Fig. 4. Finite element model of RC slab

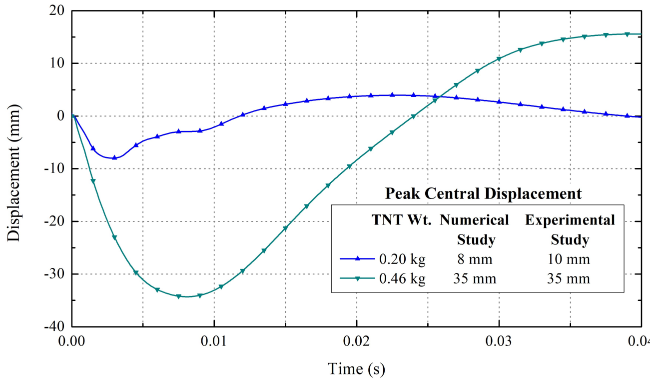


Fig. 5. Comparison of peak displacement of RC slab obtained from numerical study and experimental study [9]

## 4. Validation of developed FE approach

For the present numerical investigation, a Multi-Material Arbitrary Lagrangian-Eulerian (MM-ALE) approach is developed. To gain confidence in the accuracy of this approach, it is validated with experimental data reported by Wang et al. [10]. The study included experimental blast tests on 1 m × 1 m × 40 mm reinforced concrete slab. The study reported a peak central deflection of10 mm and 35 mm for airbursts of 0.20 kg and 0.46 kg yields (TNT equivalent), respectively. The experimental setup is numerically simulated for the corresponding explosive yields as illustrated in Fig. 4. The displacement time history depicted in Fig. 5 is generated using numerical simulation and is in good agreement with the findings of experiments, confirming the validity of the FE approach.

## 5. Results and Discussions

For each case of the investigation, a 50 kg explosive (TNT equivalent) is detonated at the mouth of the tunnel. Wave propagation through the tunnel is studied by analyzing the pressure distribution inside the tunnel at different time instants from the time of detonation, as presented in Fig. 6. On detonation of explosive a spherical wave is created. Since the explosive is located at the symmetrical end of the tunnel, hemispherical waveform can be seen in the figure.

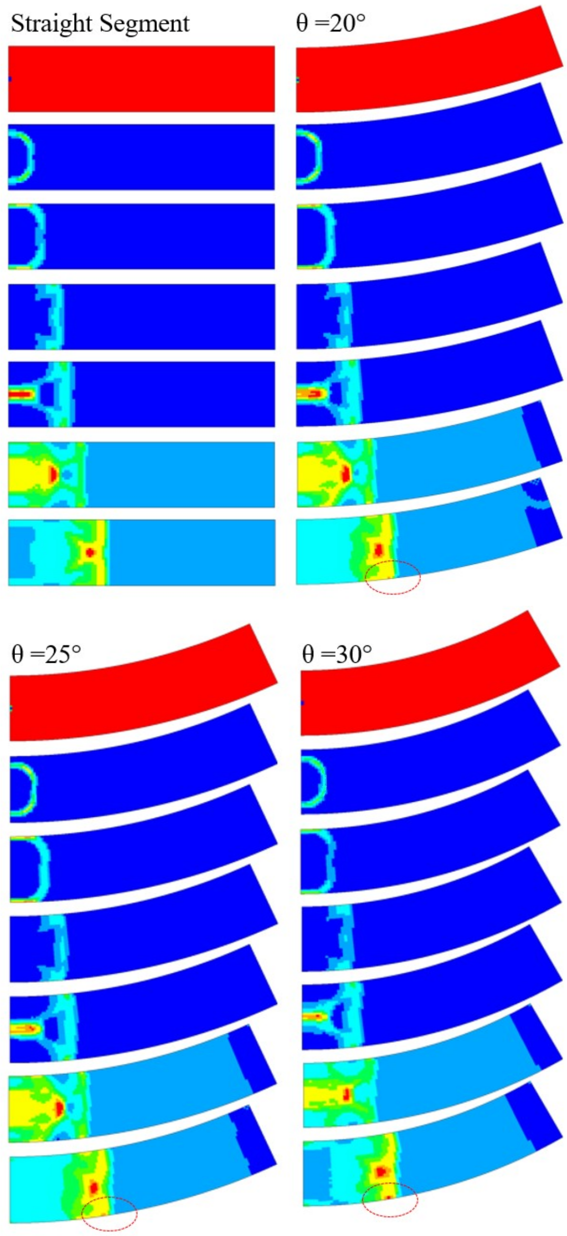


Fig. 6. Blast Wave propagation along the length of the tunnel with varying angles of curvature

The wave radially expands and collides with the inner tunnel walls. On interaction with the walls, reflected shock waves are created on either side of the tunnel. These reflected waves travels inward and later coalesces together creating a region of higher pressure along the centre line of the tunnel. This merging leads to generation of another wave which seems to have higher pressure magnitude and velocity. It can be seen in the figure that the incident wave takes the form of a planar front, followed by a near-spherical wave behind it, which is the newly formed wave after the coalescence. Due to the higher velocity of the following spherical wave, it soon catches up with the planar wave. This causes another merging of waves and forming another

Pocket of higher pressure near the tunnel lining. The multiple reflections of waves continuously occur inside the tunnel. But as the waves propagate further their intensity decreases due to attenuation. This phenomenon is observed in each case considered; however, the reflection pattern and intensity of pressure differ due to the change in the angle of curvature of the tunnel.

For a straight tunnel segment, the initial angle of incidence of wave is found to be between 35-40°. A symmetrical pattern can be observed as the wave propagates inside the tunnel. The pressure is higher in the initial section of the tunnel and then it gradually decreases as the waves travel further along the tunnel length. Whereas, the wave propagation observed in curved tunnels is asymmetrical. Introducing curvature leads to concavity and convexity of the tunnel wall. As the angle of curvature is increased the angle of incidence for the concave wall decreases, whereas the angle of incidence for the convex wall increases. A decrease in the angle of incidence leads to an increase in the magnitude of reflected pressure [11]. This explains the increase in pressure on the concave side of the tunnel, as well as, the increase in said pressure as the angle of curvature of the tunnel is increased, as observed in Fig. 6.

Further detailed analysis of the effect of curvature on the blast pressure acting on the tunnel and the response of the tunnel is carried out. This is done by comparing the pressure, peak particle velocity, and von-Mises stress on the inner side of a straight tunnel segment and curved tunnel with θ = 30°. The peak value of each parameter is taken from the walls along the length of the tunnel and plotted.

The comparison in terms of peak pressure is presented in Fig. 7. The peak pressures measured from the wall of a straight tunnel and the convex wall of curved tunnel are comparably in the same range. However, the peak pressures measured from the concave wall of the curved tunnel are vastly different.

A steep increase in the peak pressure is observed for the tunnel length from 3 m to 6 m. The increase in pressure is almost by a factor of 2. This could be because the blast wave's angle of incidence was less when it contacted the concave wall at this section of the tunnel. This increase is similarly observed in the blast wave propagation illustrated in Fig. 6.

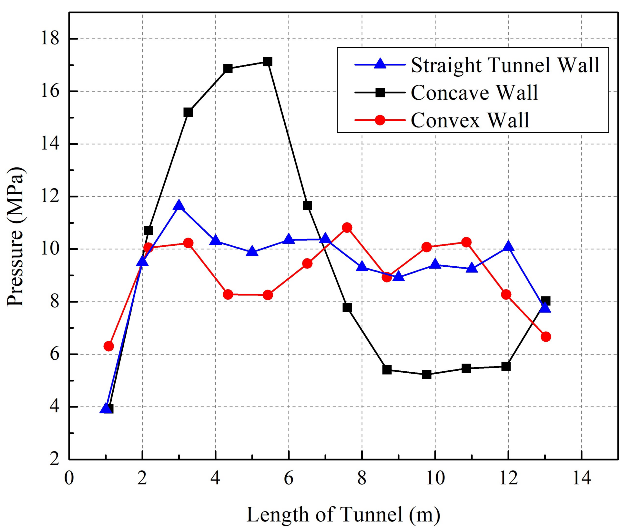


Fig. 7. Comparison of peak pressure observed on the tunnel walls of straight tunnel segment and curved tunnel segment with θ = 30°

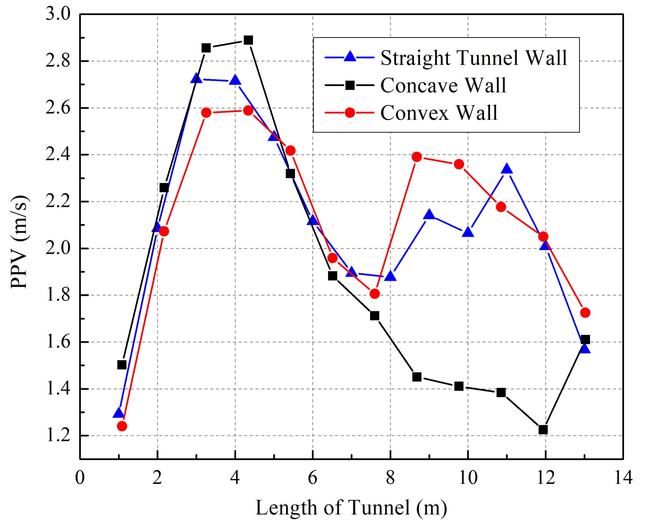


Fig. 8. Comparison of PPV observed on the tunnel walls of straight tunnel segment and curved tunnel segment with θ = 30°

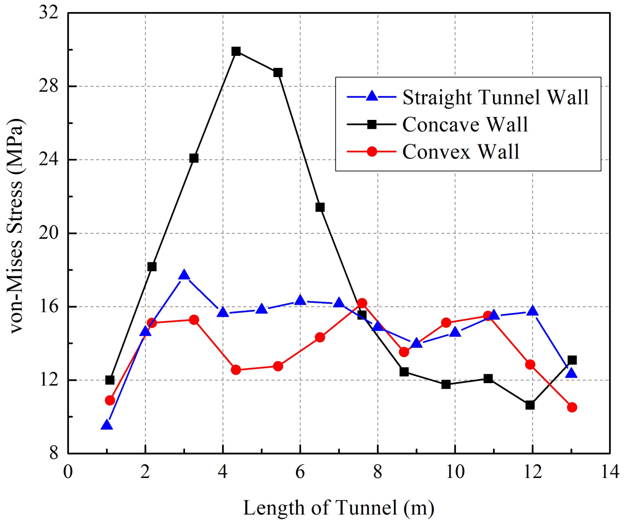


Fig. 9. Comparison of von-Mises stress observed on the tunnel walls of straight tunnel segment and curved tunnel segment with θ = 30°

Similarly, an increase in the response of the tunnel in terms of peak particle velocity and von-Mises stress is observed for the same stretch of the concave wall of the curved tunnel, as seen in Fig. 8 and Fig. 9, respectively. This implies that the introduction of curvature increases the damage susceptibility of certain sections of tunnel than other parts.

As the distance increases from the point of explosion, a decline in pressure and response parameters are observed with the concave wall showing a greater reduction in their values.

## 6. Conclusions

The effect of change in horizontal curvature of the tunnel on the blast wave propagation and dynamic response of tunnel under internal explosion was studied using finite element method. The problem was modeled using the MM-ALE technique which is suitable for simulating fluid-structure interaction under high strain rate loading. Three angles of curvature were chosen for the study: θ = 20°, 25°, and 30°.

The blast wave propagation and the response of tunnel of curved tunnels are compared with that of a straight segment of tunnel. The findings of the study are listed below:

1. Multiple reflections of blast waves were observed in all the cases considered. The sequence of formation of reflected waves was similar, however, great variation in the pattern of blast wave propagation was observed as the angle of curvature of the tunnel was increased.
2. Higher peak pressures were recorded on the concave wall of the tunnel compared to the convex wall of a curved tunnel and the wall of the straight segment of tunnel. The increase in pressure was almost by a factor of 2.
3. An increase in the response of the tunnel was observed with an increase in the angle of curvature. The PPV measured on the concave wall of curved tunnel was found to be higher than that measured on the convex wall and straight tunnel's wall. Although the difference in PPV was not much, a significant increase in the von-Mises stress at a stretch of 3 m - 6 m of the tunnel on the concave side was seen. This could be because the angle of incidence of the blast wave was smaller when the wave hit the concave wall in this stretch of the tunnel. This suggests that some tunnel sections are more vulnerable to damage than others when curvature is introduced.

## Disclosures

Free Access to this article is sponsored by SARL ALPHA CRISTO INDUSTRIAL.

### References

1. Kristoffersen M, Minoretti A, Børvik T. On the internal blast loading of submerged floating tunnels in concrete with circular and rectangular cross-sections. Engineering Failure Analysis, 2019, 103(May), 462–480.
2. Liu H. Soil-Structure Interaction and Failure of Cast-Iron Subway Tunnels Subjected to Medium Internal Blast Loading. Journal of Performance of Constructed Facilities, 2012, 26(5), 691–701.
3. Tiwari R, Chakraborty T, Matsagar V. Dynamic Analysis of Tunnel in Weathered Rock Subjected to Internal Blast Loading. Rock Mechanics and Rock Engineering, 2016, 49(11), 4441–4458.
4. Uystepruyst D, Monnoyer F. A numerical study of the evolution of the blast wave shape in rectangular tunnels. Journal of Loss Prevention in the Process Industries, 2014, 34, 225–231.
5. Yu H, Wang Z, Yuan Y, Li W. Numerical analysis of internal blast effects on underground tunnel in soils. Structure and Infrastructure Engineering, 2016, 12(9), 1090–1105.
6. Livermore Software Technology Corporation (LSTC), LS-DYNA Keyword User's Manual, Version 971 R10.1.0, 2018.
7. Bassan S. Sight distance and horizontal curve aspects in the design of road tunnels vs. highways. Tunnelling and Underground Space Technology, 2015, 45 (2015): 214-226.
8. Mussa MH, Mutalib AA, Hamid R, Naidu SR, Radzi NAM, Abedini M. Assessment of damage to an underground box tunnel by a surface explosion. Tunnelling and Underground Space Technology, 2017, 66(November 2016), 64–76.
9. Mandal J, Agarwal AK, Goel MD. Numerical Modeling of Shallow Buried Tunnel Subject to Surface Blast Loading. Journal of Performance of Constructed Facilities, 2020, 34(6), 04020106.
10. Wang W, Zhang D, Lu F, Wang S, Tang F. Experimental study and numerical simulation of the damage mode of a square reinforced concrete slab under close-in explosion. Engineering Failure Analysis, 2013, 27, 41-51.
11. Goel MD, Matsagar VA. Blast-Resistant Design of Structures, Practice Periodical on Structural Design and Construction, 2014, 19, 04014007.